Band-edge alignment of SiGe/Si quantum wells and SiGe/Si self-assembled islands

M. El Kurdi,* S. Sauvage, G. Fishman, and P. Boucaud

Institut d'Électronique Fondamentale, UMR CNRS 8622, Bâtiment 220, Université Paris Sud, 91405 Orsay Cedex, France

We report on the energy band gap and band lineup of SiGe/Si heterostructures either in the case of coherently strained quantum wells or in the case of SiGe/Si self-assembled islands. We take into account the strain field and the quantum confinement effects through an accurate description of the conduction band including the Δ and L bands. The strain field is calculated using a microscopic valence force field theory. The conduction-band diagram and energies are obtained from a 30-band $\mathbf{k} \cdot \mathbf{p}$ Hamiltonian accounting for the strain through the Bir-Pikus Hamiltonian. The band-edge description is first given for biaxially strained pseudomorphic SiGe layers. In SiGe quantum wells grown on relaxed silicon, the band line-up switches from type I to type II depending on the value of the average valence band offset. Applying the 30-band formalism to the case of heterostructures grown on relaxed silicon germanium buffer layers indicates that a better agreement with experimental data is obtained for a valence-band offset value $\Delta E_v = 0.54x$ where x is the Ge composition. For this parameter, a type-II band lineup is thus expected for all compositions of pseudomorphic SiGe/relaxed Si heterostructures. For GeSi/Si islands, we take into account the strain relaxation in the surrounding Si matrix. A type-II band lineup is predicted for all Ge compositions. The near-infrared interband recombination energy of the islands is calculated as a function of their SiGe composition.

PACS number(s): 73.21.La, 73.21.Fg, 78.20.Bh, 78.67.De

I. INTRODUCTION

Silicon germanium (SiGe) heterostructures on Si are now widely used in microelectronics and photonic devices. The band-gap energy as well as the valence- and conduction-band discontinuities are among the main parameters to describe the heterostructures. In the case of compressively strained SiGe on Si(100), i.e., a tetragonally distorted alloy with a lateral lattice constant equal to the bulk silicon lattice constant, a large band discontinuity is observed in the valence band with an offset around 7 meV per percent of germanium in the alloy.[1] The situation is less clear for the conduction band since different types of band lineup have been reported in the literature.[1–9] The biaxial strain lifts the degeneracy of the six conduction Δ valleys, the energy of the four valleys $\Delta 4$ in the layer plane being lowered while the energy of the two valleys in the growth direction $\Delta 2$ is raised. The position of the $\Delta 4$ valleys of the SiGe alloy above or below the six degenerate Δ valleys in silicon remains controversial. Experimentally, a type-I band lineup (i.e., electrons and holes confined in the SiGe alloy) has been reported for compressively strained SiGe quantumwells (QWs) by Fukatsu *et al.*[2] and by Houghton *et al.*[3] from photoluminescence experiments under an external applied stress. On the contrary, a type-II band alignment (i.e., holes confined in the SiGe layer and electrons confined in the Si matrix) was reported by Wachter *et al.*[4] and Baier *et al.*[5] Thewalt *et al.*[6] have argued that the reported type-I observations were due to optically induced band bending effects which are important in these heterostructures because of long recombination lifetimes. By performing optical experiments at very low excitation density in high-purity samples, Thewalt *et al.*[6] have concluded that the band alignment for $Si_{0.7}Ge_{0.3}$/Si quantum wells was of type-II origin. Theoretically, a type-I band alignment was first reported by People *et al.*[7] and Van De Walle *et al.*[1] while Rieger *et al.* did report a type-II band alignment for all ger-

manium fractions using a pseudopotential theory.[8] In all cases, the conduction-band discontinuities were small and of the order of a few meV. The comparison between theory and experiments is also not straightforward since many effects need to be taken into account for comparison including band bending, band filling, and corrections associated with exciton binding energy.

In the case of Ge/Si self-assembled islands, the tensile strain of the surrounding Si matrix needs to be taken into account. The tensile strain lifts the degeneracy between the sixfold-degenerate Δ valleys of silicon into $\Delta 2$ and $\Delta 4$ valleys. Using linear deformation potential theory, Schmidt *et al.*[9] have concluded that the $\Delta 2$ valleys in the silicon constitute the conduction-band minimum for pure Ge islands. In Ref. 9, the valence-band shifts were obtained from the linear deformation theory[10] and the band lineup was deduced by taking into account the known values of the material band gaps. The electronic confinement in the Δ valleys was not taken into account. For a proper analysis of experiments and device simulation, the conduction- and valence-band states need to be described accurately. This description can be obtained using a multiband $\mathbf{k} \cdot \mathbf{p}$ formalism which allows to describe simultaneously both the band alignment type and the resulting confinement of electron and hole states beyond the effective mass approach. The discussion on the band lineup of SiGe/Si heterostructures requires also an accurate description of the strain field and needs to account for the influence of strain on the band structure associated with diagonal and nondiagonal elements.

In this article, we report on the band-gap energies and band lineup of SiGe/Si heterostructures. Compressively strained QWs or self-assembled islands are considered. The energy diagram is obtained through a 30-band $\mathbf{k} \cdot \mathbf{p}$ formalism which provides a description of the conduction band all over the Brillouin zone, including the Δ and L valleys.[11] The 30-band $\mathbf{k} \cdot \mathbf{p}$ method which takes into account band mixing and nonparabolicity effects is to our knowledge applied for

the first time to calculate simultaneously the conduction- and valence-band states of SiGe islands. The strain field is calculated using a three-dimensional (3D) valence force field microscopic theory. The strain influence on the energy diagram is introduced through the Bir-Pikus Hamiltonian, thus providing a good description of the coupling between the different bands through off-diagonal matrix elements. The quantum confinement is calculated by solving the 1D Schrödinger equation. This approach is obviously valid for quantum wells. In the case of Ge/Si self-assembled islands, the calculation of strain fields are performed for dome (i.e., lens-shaped) geometries with a small aspect ratio (height divided by base length). The main confinement stems from the z direction while a large thickness is observed in the layer plane, and the islands can be in a reasonable approximation described by an equivalent quantum well. The case of pyramidal islands or hut geometries with small sizes, where the strain field can exhibit very strong variations at the apex of the pyramids, would require a three-dimensional electronic description. The 3D description of such structures with a 30 band $\mathbf{k} \cdot \mathbf{p}$ formalism is, however, beyond the scope of this article.

In the case of biaxially strained pseudomorphic quantum wells on Si(100), a type-II or type-I band alignment is found depending on the Ge composition and on the input parameters taken from the literature. In the case of type-I alignment where the conduction-band minimum is given by the $\Delta 4$ valleys, a weak electronic potential confinement is calculated with a large spreading of the wave functions in the barrier. We show that the conduction-band alignment depends on the valence-band offset magnitude. The average valence-band offset calculated by Van De Walle *et al.*,[1] $\Delta E_V = 0.54x$ (eV) leads to a systematic type-II conduction-band alignment while the relation given by Colombo *et al.*,[20] $\Delta E_V = 0.47x$ leads to a type-I (type-II) conduction-band alignment for $x < 0.7$ ($x > 0.7$). This result is in contrast with previous works, like the theoretical work of Rieger *et al.*[8] where a valence-band offset $\Delta E_V = 0.47x$ is considered, and where only type-II alignment was predicted whatever the Ge composition in the strained layer. The 30-band formalism applied to the case of heterostructures grown on relaxed buffer layers indicates that the valence-band offset of $0.54x$ is more adequate to describe the heterostructures, i.e., a systematic type-II alignment is predicted in this case for all Ge compositions of strained SiGe layers grown on relaxed Si.

In the case of GeSi self-assembled islands embedded in Si, the strain in the barrier makes the band alignment different from the pseudomorphic case. The tensile strain in the barrier material induces a splitting of the Δ valleys with $\Delta 2$ valleys constituting the lower conduction-band edge. On the other hand, the compressive strain in the island induces an opposite splitting with the $\Delta 4$ valleys constituting the lower band edge in the GeSi layer. The $\Delta 2$ valleys in the barrier constitute the lower band edge for electrons, leading to a type-II alignment, independently of the Ge composition.

The article is organized as follows. Section II presents the 30-band $\mathbf{k} \cdot \mathbf{p}$ formalism and the strain Hamiltonian of Bir and Pikus. We discuss the values of input parameters used in the calculations and we give a set of local (in $\mathbf{k}$ space) strain potential values for the Δ valleys in Si and Ge. The energy band gap and the band lineup for biaxially strained quantum wells are presented in Sec. III. Section IV deals with the case of self-assembled islands, by accounting for the strain relaxation in the surrounding Si matrix.

II. THE 30-BAND k·p FORMALISM

Six-[12] and 14-band[13] $\mathbf{k} \cdot \mathbf{p}$ Hamiltonians allow a description of the valence-band states of SiGe heterostructures. The 30-band $\mathbf{k} \cdot \mathbf{p}$ Hamiltonian allows one to describe simultaneously the conduction- and the valence-band states all over the Brillouin zone. We show that this Hamiltonian is suited to describe simultaneously the band lineup in SiGe/Si heterostructures and the confined energy levels and wave functions in a single and consistent formalism. The method is useful to calculate the confinement energies of electron and hole states, beyond the effective mass approximation, and for the calculation of matrix elements involving the different bands. As compared to previous theoretical work, there is no need to introduce with the 30-band $\mathbf{k} \cdot \mathbf{p}$ modeling an additional procedure using the local (in $\mathbf{k}$ space) deformation potentials Ξ_u^Δ and $\left(\Xi_d^\Delta + \frac{1}{3}\Xi_u^\Delta - a_\Gamma\right)$ to deduce the band edge alignment[9,22] and to solve afterward the Schrödinger equation in an effective mass approximation.[14]

In a first step, using a 15×15 $\mathbf{k} \cdot \mathbf{p}$ Hamiltonian which does not account for spin-orbit interaction, Cardona and Pollak[15] described the dispersion curve of Si and Ge over the whole Brillouin zone. The 15-function basis used has been shown to be self-contained as far as the valence band and the first two conduction bands are concerned. The dispersion curves were described without taking into account the influence of states outside the 15-function basis. However, while in Si the spin-orbit interaction may be neglected, this approximation is less satisfying for Ge for which the spin-orbit energy splitting is more than 20% of the gap energy. Starting from the 15×15 $\mathbf{k} \cdot \mathbf{p}$ Hamiltonian, a 30-band $\mathbf{k} \cdot \mathbf{p}$ Hamiltonian has recently been developed[11] to account for the spin-orbit coupling, thus leading to better accuracy of the band description.

The set of functions and parameters involved in the 30×30 $\mathbf{k} \cdot \mathbf{p}$ Hamiltonian are given in Fig. 1. The energy levels at $\mathbf{k} = 0$ and the matrix elements of the momentum operator p used in the 30-band model for Si and Ge can be found in Ref. 11, and are recalled in Table I. A linear interpolation is made on the $\mathbf{k} \cdot \mathbf{p}$ matrix elements for Si and Ge to obtain the band diagram description of $Si_{1-x}Ge_x$ alloys. Following Ref. 16, a linear interpolation can be made for the band energy at the Γ point. A quadratic interpolation is used for the Γ_4^- and Γ_2^- bands in order to reproduce the quadratic behavior of the Δ valley energies as reported in Ref. 17, noting that the Δ valleys stem from these two bands in the double group (i.e., Γ_7^-, Γ_6^-, Γ_8^-). Concerning the lattice constant parameters, a very weak deviation from a linear law has been reported in the literature for SiGe bulk materials.[18] This deviation is neglected in this work. Concerning elastic constants, a linear relationship with composition is assumed following Ref. 19. Most calculations of band-edge alignment in the 30×30 $\mathbf{k} \cdot \mathbf{p}$ formalism uses the average valence-band offset calculated by Colombo *et al.*,[20] $\Delta V_{av} = 0.47x$.
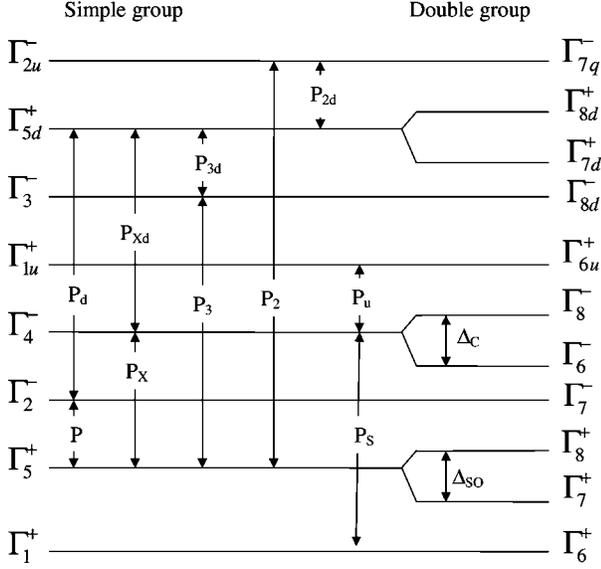
FIG. 1. O_h group bands involved in the 15-band $\mathbf{k} \cdot \mathbf{p}$ model for simple group used by Cardona and Pollak (Ref. 15) and for double group used in the 30-band model at $\mathbf{k} = 0$ (center of the Brillouin zone) in the Koster notation. (Ref. 31). The momentum matrix elements P_i which are used in the 30-band model are defined in Ref. 11.

The Bir-Pikus strain Hamiltonian is included in the electronic-state calculation to account for the strain potential following the procedure described in Refs. 10,21. The values of the zone center deformation potential used in the strain Hamiltonian of Bir and Pikus[10] $(b_{\Gamma_4^-}, b_{\Gamma_5^+}, a_{\Gamma_4^-}, a_{\Gamma_2^-}, a_{5V})$, given in Table II, are taken from the literature except for the local deformation potential values Ξ_u^Δ and $(\Xi_d^\Delta + \frac{1}{3}\Xi_u^\Delta - a_\Gamma)$ discussed in the following, and for the splitting deformation

TABLE I. Kane momentum matrix element values E_{P_i} (in eV) used in the 30-band model and related to the momentum operator p matrix element P_i (see Fig. 1) by the relation $E_{P_i} = (2m_0/\hbar^2)(P_i)^2$ with m_0 the free-electron mass and $\hbar$ the reduced Planck constant. Spin-orbit splitting energy in eV involved in the 30-band $\mathbf{k} \cdot \mathbf{p}$ model for Si and Ge. A linear interpolation on the parameters used for Si and Ge is made to provide SiGe alloy band parameters.

Parameter	Si	Ge
Δ_{SO}	0.044	0.290
Δ_C	0	0.21
E_P	19.96	24.6
E_{P_X}	14.81	17.65
E_{P_3}	4.475	5.212
E_{P_2}	3.993	2.51
E_{P_S}	1.092	1.071
E_{P_d}	1.193	0.0051
$E_{P_{Xd}}$	7.491	12.23
$E_{P_{3d}}$	9.856	15.76
$E_{P_{2d}}$	20.76	27.59
E_{P_u}	16.36	17.84

potential $b_{\Gamma_4^-}$ of the conduction band Γ_4^-. The $b_{\Gamma_4^-}$ parameter for Si is adjusted to match the conduction-band energy splitting of strained Si on relaxed $Si_{1-x}Ge_x$, $E_{\Delta2} - E_{\Delta4} = 0.67x$, given by Ref. 22. For Ge, the $b_{\Gamma_4^-}$ parameter is adjusted to match the band-gap energy of strained $Si_{1-x}Ge_x$ on relaxed Si as measured in Ref. 23. Since the $b_{\Gamma_4^-}$ values have not been reported in the literature except for a 20-band $\mathbf{k} \cdot \mathbf{p}$ formalism,[21] the value deduced for the local deformation potentials for the Δ valleys is compared to the values usually used in the calculation of conduction-band lineups.

First we have computed the band diagram of strained Si on SiGe and Ge on SiGe for various SiGe alloy compositions. We then extract the strain-induced band-gap energy variation $E_{\Delta4} - E_{lh}$ $(E_{\Delta4} - E_{hh})$ of strained $Si/Si_{1-x}Ge_x$ $(Ge/Si_{1-x}Ge_x)$ and the conduction-band splitting $E_{\Delta2} - E_{\Delta4}$. To deduce the local deformation at the Δ valleys we apply a fit procedure using the following set of equations:[21]

$$E_{\Delta2} - E_{\Delta4} = \Xi_u^\Delta \times \varepsilon_{II\perp} \quad \text{with } \varepsilon_{II\perp} = \varepsilon_{zz} - \varepsilon_{xx}, \quad (1)$$

$$E_{\Delta2} - E_{lh} = \left(\Xi_d^\Delta + \frac{1}{3}\Xi_u^\Delta - a_{\Gamma_4^-}\right)\varepsilon + \frac{2}{3}\Xi_u^\Delta \varepsilon_{II\perp} - \frac{1}{2}\left[b_{\Gamma5v}\varepsilon_{II\perp} \right.$$
$$\left. - \Delta + \sqrt{(\Delta + b_{\Gamma5v}\varepsilon_{II\perp})^2 + 8(b_{\Gamma5v}\varepsilon_{II\perp})^2}\right], \quad (2)$$

$$E_{\Delta4} - E_{hh} = \left(\Xi_d^\Delta + \frac{1}{3}\Xi_u^\Delta - a_{\Gamma_4^-}\right)\varepsilon - \frac{1}{3}\Xi_u^\Delta \varepsilon_{II\perp} - b_{\Gamma5v}\varepsilon_{II\perp}. \quad (3)$$

For both cases, i.e., Si on $Si_{1-x}Ge_x$ and Ge on $Si_{1-x}Ge_x$, the extracted values of local deformation potential are weakly dependent on the composition of the unstrained substrate, indicating a small uncertainty, by about 10% of the potential energies. The $(\Xi_d^\Delta + \frac{1}{3}\Xi_u^\Delta - a_{\Gamma_4^-})$ potential value deduced from the $\mathbf{k} \cdot \mathbf{p}$ method, as shown in Table II, falls into the range of data published for both Si and Ge.[24] The Ξ_u^Δ value of 9.1 eV for Si is also in agreement with the magnitude given in the literature.[25,26] In the case of Ge, we obtain a Ξ_u^Δ value of 17.3 eV, which is large as compared to values reported in the literature. The resulting $E_{\Delta2} - E_{\Delta4}$ energy splitting for SiGe strained alloys on Si is large as compared to data reported by other groups but is, however, consistent with the $b_{\Gamma_4^-}$ value that we have adjusted for Ge to match the experimental band-gap energy of strained SiGe/Si layers.

III. PSEUDOMORPHICALLY STRAINED SiGe LAYERS ON RELAXED Si

The calculated energy-band gap of a pseudomorphically strained SiGe layer is reported in Fig. 2 which also shows the experimental data of Ref. 23 and the calculated energy gap of Ref. 8. Since we have adjusted the $b_{\Gamma_4^-}$ parameter to match one experimental data point of Ref. 23 (at $x = 0.5$), the band-gap energy obtained by our calculation for other germanium average compositions remains in good agreement with the data of Ref. 23. The theoretical values of Ref. 8 shown in Fig. 2 deviate significantly from our results and those reported by Lang and People.[23] For the case of pure strained

TABLE II. Local (in the Δ valleys) and Brillouin Zone center strain potentials (in eV) of Bir and Pikus for Si and Ge.

	Ξ_u^Δ	$(\Xi_d^\Delta + \frac{1}{3}\Xi_u^\Delta - a_{\Gamma_4^-})$	$b_{\Gamma_5^+}$	$b_{\Gamma_4^-}$	$a_{\Gamma_2^-}$	$a_{\Gamma_4^-}$	a_{5V}
Si	9.1,[a] 10.5,[b] 9.29,[c] 9.2[d]	−0.18,[a] 2.5,[b] 0.29,[c] −0.179[d]	2.35[e]	−5.05,[a]–8.8[d]	−5.1[f]	−0.2[f]	0
Ge	17.3,[a] −9.75,[b] 10.2[c]	−2.4,[a] −5.75,[b] −1.9[c]	2.55[e]	−9.5[a]	−8.8[f]	−8.9[f]	0

[a]Present work.
[b]Reference 26.
[c]Reference 8.
[d]Reference 21.
[e]Reference 1.
[f]Reference 32.

Ge on relaxed Si, the gap energy using the 30-band $\mathbf{k}\cdot\mathbf{p}$ formalism is lowered by about 100 meV as compared to the one reported by Ref. 8. However we can note that the band-gap energy at low temperature of 0.74 eV for bulk unstrained Ge obtained with the 30-band $\mathbf{k}\cdot\mathbf{p}$ formalism is in good agreement with the energy gap calculated by Rieger *et al.*[8] in a nonlocal pseudopotential theory. It is in addition in good agreement with the experimental band-gap energy reported in Ref. 27.

Figure 3(a) shows the energies of the Δ and L conduction valleys and Fig. 3(b) shows the valence-band edges in the strained $Si_{1-x}Ge_x$ layer, obtained with the $\mathbf{k}\cdot\mathbf{p}$ formalism and including an average band offset in the valence band of $\Delta V_{av}=0.47x$.[20] The origin of the energies is taken at the edge of the valence band of the Si substrate and the values at $x=0$ in Figs. 3(a) and 3(b) correspond to the energy of the band edge of pure unstrained silicon. The band lineup of the Δ and L conduction bands and of the valence bands for strained $Si_{1-x}Ge_x$ on unstrained Si can thus be deduced from the data reported in Fig. 3. Note that the band lineup of the L valley (not shown) and the corresponding electronic states will not be considered as they are, for all Ge compositions, at higher energy than the Δ valleys for both the Si barrier and the SiGe layer. As shown in Fig. 3(b), the strain induces a splitting in the valence band between heavy holes (hh) and light holes (lh), and the hh band constitutes the upper band edge. The total valence-band offset $\Delta E_V = E_{hh}^{SiGe} - E_{hh}^{Si}$ (we take $E_{hh}^{Si}=0$) follows a linear dependence on the germanium composition. By taking the average valence-band offset of

$\Delta V_{av}=0.47x$, the computed valence-band offset may be expressed by $\Delta E_V=0.73x$. As shown in Fig. 3(a), the strain induces a splitting of the Δ valleys into fourfold- and twofold-degenerate valleys, $\Delta 4$ and $\Delta 2$, respectively. The large splitting $E_{\Delta 2}-E_{\Delta 4}$ reported in Fig. 3(a) as compared to data published in the literature is the consequence of the choice of the adjustment procedure of the Bir-Pikus deformation potential $b_{\Gamma_4^-}$. In the case of compressive strain, the fourfold-degenerate valleys $\Delta 4$ constitute the lower band edge in the conduction band. To describe the fundamental conduction-band states in a pseudomorphically strained SiGe layer on Si, the band alignment of interest involves the band offset between the Δ valleys in Si and the $\Delta 4$ valleys in the strained SiGe layer, $\Delta E_C = E_{\Delta 4}^{strained\ SiGe} - E_{\Delta}^{cubic\ Si}$. As commonly obtained by other studies, the $\mathbf{k}\cdot\mathbf{p}$ formalism gives a
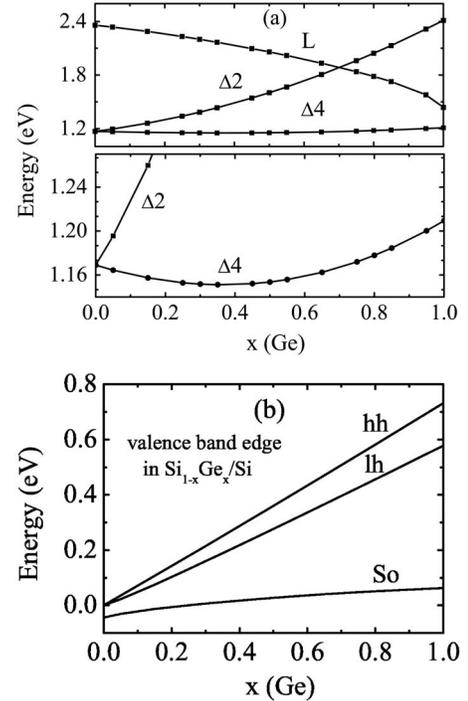
FIG. 3. (a) Conduction-band edges in the Δ and L valleys. The lower part of the figure is a zoom at low energy to highlight the difference between the split $\Delta 2$ and $\Delta 4$ valleys. (b) Valence-band edges for pseudomorphically strained $Si_{1-x}Ge_x$ on unstrained Si calculated using the $\mathbf{k}\cdot\mathbf{p}$ formalism uncluding strain via the Bir-Pikus Hamiltonian. The band edges at $x=0$ correspond to those of the unstrained Si substrate with the valence-band edge taken as energy origin.

FIG. 2. Fundamental band-gap energy of strained SiGe/Si calculated within the framework of 30-band $\mathbf{k}\cdot\mathbf{p}$ model (full line). The data reported in Ref. 8 (triangles) and in Ref. 23 (full dots) are given as comparison.

very small band offset ΔE_C in the Δ valleys and most of the band-gap discontinuity is in the valence band, i.e., $\Delta E_V \gg \Delta E_C$. This small conduction-band offset makes ambiguous the determination of type-I or type-II band alignment, which remains a controversial issue in the literature. Our results show that both type-I and type-II band alignments occur in the system depending on the germanium composition. For $x<0.7$ the bands are aligned as type I ($\Delta E_C<0$) and for $x>0.7$ the band alignment is found to be type II ($\Delta E_C>0$) for a given average valence-band offset $\Delta V_{av}=0.47x$ eV.[20] These results are in agreement with band lineups deduced in both theoretical and experimental studies.[2,3,7] The conduction-band offset $\Delta E_C=-17$ meV obtained in the $\Delta 4$ valleys for a strained $Si_{0.5}Ge_{0.5}$ layer on a cubic silicon substrate can be compared to the result obtained in Ref. 7, $\Delta E_C=-20$ meV. However, several studies[5,6] have claimed a type-II alignment if the substrate is unstrained Si, following the theoretical article of Rieger *et al.*[8] in which a type-II alignment over the whole range of x was predicted. We can note that in the theoretical work of Ref. 8, the computation of the band offset uses the same average valence-band offset as in this work, $\Delta V_{av}=0.47x$.[20] Since the band offset in the conduction band is very small, it will be very sensitive to the input parameters. We have performed the calculation of the band-edge alignment by considering other input parameters from the literature. For example, if we use a larger average valence-band offset $\Delta V_{av}=0.54x$ eV as calculated by Van De Walle *et al.*,[1] the Γ_4^- band in SiGe shifts to higher energy as compared to Γ_4^- in the Si substrate since the direct energy gap Γ_4^--Γ_5^+ in the strained layer will not change with ΔV_{av}. As the $\Delta 4$ valleys in SiGe are built from the Γ_4^- branch, a shift of this valley to higher energy and thus a band alignment modification can be predicted at the SiGe/Si interface. In the case of $\Delta V_{av}=0.54x$ eV, we find that the band alignment for the $\Delta 4$ valleys remains type II for all Ge compositions as predicted by Rieger *et al.*[8] and observed experimentally by Thewalt *et al.*[6] The magnitude of the calculated band offset is similar in this case to the one given in Ref. 8. For example, if we take $\Delta V_{av}=0.54x$ for a strained $Si_{0.4}Ge_{0.6}$/Si quantum well, we obtain a type-II conduction-band offset of 30 meV which can be compared with the 20 meV value given in Ref. 8. We emphasize that even in the framework of a 30-band $\mathbf{k} \cdot \mathbf{p}$ model the theoretical determination of type-I or type-II conduction-band lineup for strained silicon germanium on relaxed Si is not straightforward and the issue of electron-hole localization in this system has to be addressed experimentally. Note that, if we follow the experimental results of Ref. 6, i.e., a type-II alignment, a valence-band offset $\Delta V_{av} >0.527$ eV has to be introduced in the 30-band formalism. The 30-band formalism can obviously be applied to the case of heterostructures grown on relaxed buffer layers which are more sensitive to the values of the valence-band potential offset. In Ref. 28, Sigg *et al.* have reported photoluminescence data on strained silicon/strained silicon germanium quantum wells grown on a relaxed buffer layer. If we consider the parameters indicated in this reference and apply the 30-band $\mathbf{k} \cdot \mathbf{p}$ formalism (i.e., calculation of conduction and valence confinement energies), the electron-hole recombination energy is calculated, for a valence-band offset of $0.54x$, at 640 meV for the 70% composition sample and measured
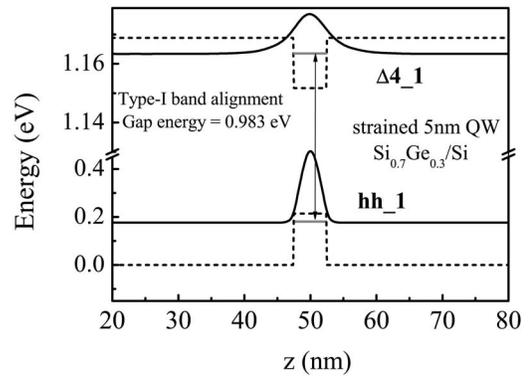
FIG. 4. Band lineup and resulting fundamental electron and hole confined levels and wave functions in strained $Si_{0.7}Ge_{0.3}$/Si quantum well with a 5 nm height, calculated within the framework of the 30-band model. The calculation uses an average valence-band offset given by Colombo *et al.* (Ref. 20). Note that the $\Delta 4$ valley lineup (in the upper part of the figure) is not represented on the same scale as the hh valley lineup (in the lower part of the figure).

experimentally at 620 meV. The agreement is thus quite good considering that the exciton binding energy and band bending effects are not taken into account. A small deviation from the nominal thickness parameters can also occur. A similar agreement is obtained for the other compositions. The deviation would be around 65 meV between calculation and experimental data if we consider a valence-band offset of $0.47x$. These results tend to indicate that the $0.54x$ valence potential offset is more appropriate to describe the SiGe heterostructures.

In the following and in order to make a comparison with values used in the theoretical work of Ref. 8, we have nonetheless performed computations with $\Delta V_{av}=0.47x$. The average band offset $\Delta V_{av}=0.54x$ is considered for the calculation of the band-gap energy of self-assembled islands (Sec. IV).

As shown in Fig. 4, for a 5-nm thick $Si_{0.7}Ge_{0.3}$ strained quantum well on Si, a type-I alignment is obtained with $\Delta V_{av}=0.47x$, and should lead to a confined state in the $\Delta 4$ valleys with electrons and holes localized in the SiGe layer. The band alignment leads to a potential confinement of 17 and 215 meV for electrons and holes, respectively. The electron confinement energy, which is roughly 12 meV, presents a weak contribution to the fundamental band-gap energy and the fundamental electron energy is at 5 meV from the barrier continuum. The fundamental electron state $\Delta 4\_1$ is weakly localized in the SiGe layer while the hole wave function of the fundamental state hh$\_1$ which is at 181 meV from the Si continuum of the barrier is more tightly confined in the well.

IV. SiGe SELF-ASSEMBLED ISLANDS IN A Si MATRIX

In this section we describe the strain-induced band lineup and the resulting confined states in self-assembled GeSi islands using the 30-band $\mathbf{k} \cdot \mathbf{p}$ formalism. The strain is calculated by minimizing the strain energy given by a microscopic valence force field theory,[29] used to calculate the crystal
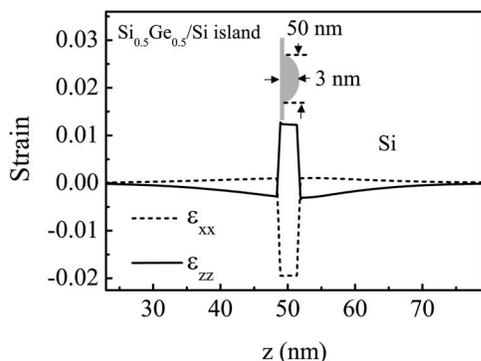
FIG. 5. Calculated strain components along the growth direction through the middle of a single island embedded in Si with 50% of Ge average composition. An island with a height of 3 nm and a base diameter of 50 nm is considered. The profile is obtained from a 3D finite-element calculation using a valence force field theory (Ref. 29).

deformation at an interatomic length scale. 17×10^6 atoms are considered, distributed in 129^3 silicon cubic unit cells $(a_{Si} \times a_{Si} \times a_{Si})$ forming a 69.5 nm^3 volume (or supercell). In order to take into account the finite Ge composition in this atom-based microscopic theory, a virtual zinc-blende crystal is considered for SiGe, exhibiting the bond stretching and bond angle bending interaction coefficients α, β corresponding to the elastic constants of the SiGe alloy. The strain tensor was calculated in the supercell by considering in-plane periodic bonding conditions. The island and the Si barrier are grown on a rigid silicon substrate. At the upper supercell edge, a crystal/air interface is considered. The interface is taken sufficiently far from the island (35 nm) for the deformation to be negligible at the interface and the deformation around the island to be unaffected by the presence of the Si/air interface. In this work, we take a three-dimensional lens-shaped geometry for the islands. We focus on this specific geometry of the islands, which is commonly observed in transmission electron microscopy.[30] The investigated islands have a 3 nm height and a 50 nm base diameter and the corresponding aspect ratio (height over diameter) is 6%. As compared to quantum wells, the strain tensor exhibits nonvanishing shear components because of the 3D nature of the quantum island geometry. The shear components are nevertheless very small near the interface of the specific island geometry considered in this work, no more than 1% of the diagonal elements ε_{ii}, mainly because of the very small aspect ratio of the dots. As in addition the shear components are involved in nondiagonal terms of the Bir-Pikus strain Hamiltonian, we will neglect them in the following. Figure 5 shows the in-plane ε_{xx} and perpendicular ε_{xx} elongation of the strain tensor for an isolated $Si_{0.5}Ge_{0.5}$ island embedded in silicon. In the island we obtain values of $\varepsilon_{xx} = -0.0197$ and $\varepsilon_{zz} = 0.0129$ while in a linear deformation theory one would obtain $\varepsilon_{xx} = -0.0192$ and $\varepsilon_{zz} = 0.0146$ for pseudomorphically strained two-dimensional $Si_{0.5}Ge_{0.5}$/Si layers. Since strain has partially relaxed elastically in SiGe islands, a crystal deformation is observed in the surrounding silicon matrix. As deduced from Fig. 5, the hydrostatic part $\varepsilon_{xx} + \varepsilon_{yy} + \varepsilon_{zz}$ of the deformation is positive in the silicon barrier, indicating that it
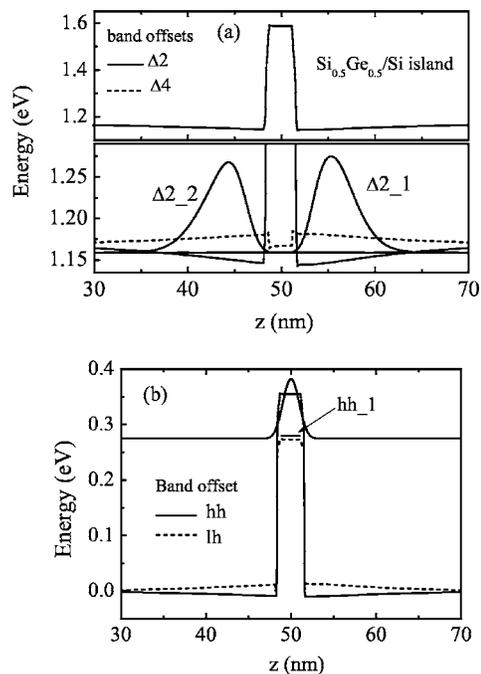
FIG. 6. (a) Band-edge alignment and confined states in the conduction band. A zoom of the conduction-band lineups is shown in the lower part of the figure. (b) Band-edge alignment in the valence band calculated using the 30-band $\mathbf{k} \cdot \mathbf{p}$ model introducing strain profile of Fig. 5, i.e., for a single $Si_{0.5}Ge_{0.5}$ island embedded in a silicon matrix. hh_1 is the ground state energy level of the heavy hole.

is under tensile strain. This induces both a Δ valley splitting and a confining potential for electrons in the barrier. The deformation is larger at the top of the island than at the bottom, by about 15%. In addition we observe a slight asymmetry of the strain slope near the SiGe/Si interface along the growth direction. As an example, the uniaxial part of the deformation $(\varepsilon_{zz} - \varepsilon_{xx})$ varies as 0.023%/nm above and 0.018%/nm below the island in the barrier material near the SiGe/Si interface. A resulting slight asymmetry of the potential experienced by the electrons is then expected.

Figures 6(a) and 6(b) show the band alignment and fundamental ground states with associated wave functions for a $Si_{0.5}Ge_{0.5}$ island embedded in silicon that are calculated in the $\mathbf{k} \cdot \mathbf{p}$ formalism using the strain profile of Fig. 5 along the growth direction. We observe that the $\Delta 4$ valleys present a type-I alignment feature $E_{\Delta 4}^{SiGe} - E_{\Delta 4}^{Si} < 0$. This is consistent with the band alignment calculated for QWs in the previous section since the SiGe layer is compressively strained for both islands and quantum wells. On the contrary, a type-II alignment occurs in the $\Delta 2$ valleys since the silicon barrier is under tensile strain. This situation cannot be obtained for pseudomorphic layers where the barriers are unstrained. The potential profile in the island thus shows simultaneously both type-I and type-II band alignment in the $\Delta 4$ and $\Delta 2$ valleys, respectively. As the band edge of the $\Delta 2$ valleys in the silicon barrier falls at lower energy than the $\Delta 4$ valleys in the islands, the fundamental ground electronic state is in the $\Delta 2$ valleys and is localized in the Si part of the SiGe/Si interface. This situation applies for the whole range of Ge compositions.

We can note that this situation remains true even if the band lineups are computed by considering an average valence-band offset $\Delta V_{av}=0.54x$ eV (not shown), since it will not change the $\Delta2$ edge lineup significantly. The potential profile experienced by electrons in $\Delta2$ is still of type II. It is not changed inside the barrier and is larger in the SiGe layer. Even if the $\Delta4$ edge is changed to type II, by taking $\Delta V_{av}=0.54x$ eV as input parameter (see the discussion in the previous section), the $\Delta2$ valleys remain the lower conduction-band edge in the barrier. As opposed to the pseudomorphic case, there is no ambiguity about the band lineup for self-assembled islands.

As shown in Fig. 6(a), the band alignment presents a confinement potential of 25 meV deep in the $\Delta2$ valleys which falls down to 0 at about 20 nm from the SiGe/Si interface. The weak asymmetry of the strain (Fig. 5) leads to an asymmetry of the potential shape for electrons. The potential seen by electrons in the $\Delta2$ valleys is weakly deeper, by about 2 meV, in the apex as compared to the bottom of the island. The fundamental level in the $\Delta2$ valleys is thus split into two levels $\Delta2\_1$ and $\Delta2\_2$, confined at the top and the bottom of the island, respectively, as compared to a case where the strain-induced confining potential would be symmetric. The difference energy between the two levels is nevertheless very small, about 1 meV.

The hole localization occurs inside the SiGe zone where the hh constitute the upper valence band. The potential height of 355 meV for holes along the growth direction through the middle of the island is not far from the one calculated in the previous section for quantum wells [ΔE_V =365 meV, Fig. 3(b)].

Figure 7(a) reports the *e-h* energy difference $E_G^{e-h}=E_{\Delta2\_1}-E_{hh\_1}$, corresponding to the energy difference between the fundamental levels $\Delta2\_1$ and hh$\_1$, for various island compositions. For all Ge average compositions in the island, the lower band edge remains in the $\Delta2$ valleys and the electron ground state is localized in the Si barrier. This was not obviously the case for 2D strained layers as discussed in the previous section. Figure 7(a) shows a quasilinear dependence of the island gap energy as a function of the Ge composition. Typical confinement energies of 5 meV are found in the $\Delta2$ valleys. This small contribution to the gap energy can be explained by the large $\Delta2$ valley masses in the z direction in Si ($m_{\Delta2}=0.917m_0$, obtained with the 30-band $\mathbf{k\cdot p}$ formalism, where m_0 is the free-electron mass) and the large penetration length of the deformation in the Si barrier, i.e., a large size of the quantum confinement potential in the Si barrier. On the other hand, the contribution of the confinement energy in the valence band to the fundamental band-gap energy is less negligible; a value of 125 meV is obtained for pure Ge islands. Holes are more confined along the z direction in the islands, i.e., the quasi quantum well seen by holes has a smaller size than the potential profile seen by electrons in $\Delta2$ valleys. Moreover, the effective mass of the hh is smaller than $m_{\Delta2}$ (a value of $m_{hh}=0.23m_0$ at the zone center is obtained with the 30-band model).

The energy difference between the valence- and conduction-band edges for the islands (i.e., without taking into account the confinement) $E_G=E_{\Delta2}^{Si}-E_{hh}^{SiGe}$ reported in Fig. 7(a) follows a linear dependence with the average Ge composi-
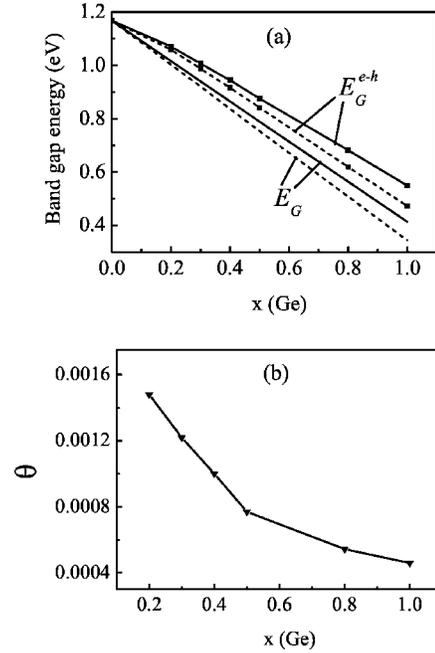
FIG. 7. (a) Calculated fundamental band gap at 0 K taking into account the confinement energy $E_G^{e-h}=E_{\Delta2\_1}-E_{hh\_1}$ (squares) and without taking into account the confinement energy $E_G=E_{\Delta2}^{Si}-E_{hh}^{SiGe}$ (full line). The values obtained in the case of an average band offset of $0.54x$ (eV) are shown in dotted lines for comparison. (b) Spatial overlap θ (see text for definition) between electrons in the $\Delta2\_1$ level and holes in the hh$\_1$ level for various Ge average compositions in the island.

tion in the islands and can be expressed as $E_G(x)=E_G^{Si}-0.76x$, where $E_G^{Si}=E_G(0)$ is the band-gap energy of unstrained bulk silicon. This can be compared with the dependence reported in Ref. 9, $E_G(x)\approx E_G^{Si}-0.71x$ (from Fig. 8 in Ref. 9) in the framework of linear deformation potential theory and using local deformation potential parameters from literature. By comparing E_G^{e-h} and E_G, we can see that the confinement energy has a non-negligible contribution (87 meV for $x=0.5$) for the island size considered in this work.

Figure 7(a) also shows in dotted lines the results obtained when considering an average band offset $\Delta V_{av}=0.54x$ as input of the 30-band $\mathbf{k\cdot p}$ calculation. The gap energy E_G still follows a linear behavior $E_G(x)=E_G^{Si}-0.825x$, which is different from the one obtained with $\Delta V_{av}=0.47x$, and deviates more significantly from the linear interpolation deduced from Ref. 9. Note that the gap energy is lowered when taking a larger valence-band offset, since in this type-II band lineup, the conduction-band edge in the barrier material is lowered with respect to the valence-band edge in the SiGe zone. The confinement energy contributions for electrons and holes are very similar to those obtained in the case of $\Delta V_{av}=0.47x$.

Figure 7(b) shows the quantity

$$\theta=\int\left[\sum_{i=1}^{i=30}|\chi_i^e(z)|^2\right]\left[\sum_{i=1}^{i=30}|\chi_i^h(z)|^2\right]dz,$$

where $\chi_i^e(z)$ are the envelope function components of the electron wave function $\psi_e=\Sigma_{i=1}^{i=30}\chi_i^e(z)u_i$ projected on the
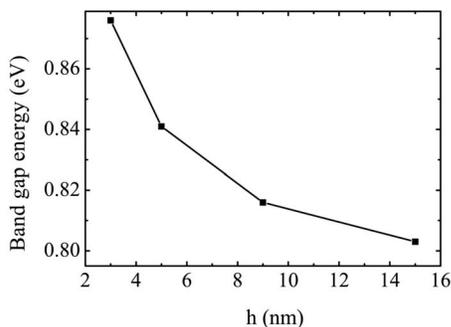
FIG. 8. Calculated interband recombination energy as a function of the island height for a 50% Ge composition. The line is a guide to the eye. A valence-band offset of $0.47x$ is considered in the calculation.

30-Bloch-function basis (u_i) and corresponding to the $\Delta2\_1$ level, while $\chi_i^h(z)$ are the envelope function components of the hole wave function $\Psi_h = \Sigma_{i=1}^{i=30} \chi_i^h(z) u_i$ corresponding to the hh_1 level. This quantity gives information on the electron-hole spatial overlap and thus on the strength of the optical recombination. The calculation of the optical oscillator strength accounting for the electron-phonon interaction in these indirect-band-gap materials (i.e., the conservation rule of the wave vector in the recombination) is beyond the scope of this article. As the Ge island composition increases, this overlap decreases and is lowered by a factor of 3 between the case of 20% composition and the case of a pure Ge island. When increasing the average Ge composition in the island, the hole wave function is more confined in the well, meaning it penetrates less into the Si barrier. The confining potential experienced by the holes is deeper, following the law $\Delta E_V = 0.71x$, which is not far from the one given in the previous section for the quantum well case ($\Delta E_V = 0.73x$). In addition, the increase of the potential experienced by electrons in the $\Delta2$ valleys with increasing x, at the SiGe/Si interface, leads to a smaller penetration length of the wave function inside the islands. The decrease of both electron tunneling inside the island and hole tunneling in the barrier with higher Ge average composition explains the decrease of the overlap factor as reported in Fig. 7(b). It shows that islands with high Ge content are not obviously the better configuration to obtain the largest electron-hole coupling, at least for the specific geometry considered in this work.

Finally, Fig. 8 shows the dependence of the interband re-

combination energy for an island with a 50% silicon germanium composition as a function of the height. The energy variation is mainly due to the change in the valence confinement energy. The interband recombination energy shifts by less than 80 meV when the thickness increases from 3 to 15 nm.

V. CONCLUSION

We have performed a calculation of the conduction- and valence-band lineups and of the electronic states for strained SiGe on Si in the two-dimensional pseudomorphic case and for self-assembled islands. This calculation was done in the framework of a 30-band $\mathbf{k} \cdot \mathbf{p}$ formalism, including the strain potential derived from a valence force field theory through the Bir-Pikus Hamiltonian. We have shown that the conduction-band lineups calculated using the $\mathbf{k} \cdot \mathbf{p}$ model are very sensitive to the average valence-band offset taken in the calculation. Even if the conduction-band alignment shows a type-I feature in the $\Delta4$ valleys, for Ge composition x lower than 0.7 and for an average band offset $\Delta V_{av} = 0.47x$,[20] the resulting electron confinement remains weak, and the corresponding wave functions are strongly coupled to the barrier. The comparison of our theoretical results with experimental photoluminescence data reported for heterostructures grown on relaxed buffer layers[28] indicates that a valence-band offset of $0.54x$ is more appropriate to describe the SiGe heterostructures. A type-II band lineup is thus expected for all Ge compositions of strained SiGe heterostructures grown on silicon. For the self-assembled island case, the issue of localization of electrons and holes is not dependent on the valence-band offset. The strain relaxation in the Si barrier leads to a confining potential for electrons at the SiGe/Si interface in the Si matrix, while holes are localized in the SiGe layer. A type-II band lineup is predicted for all average Ge compositions. The fundamental gap energies electron and hole confinement energies, and overlap have been calculated for the whole range of Ge island compositions. The interband recombination energy has also been calculated as a function of the thickness of the island. The recombination energy varies by about 500 meV when the germanium composition varies from 0 to 100%. On the contrary, the recombination energy varies by only 80 meV when the thickness increases from 3 to 15 nm. These results will be helpful to discriminate the roles of size and composition for the interpretation of self-assembled island photoluminescence spectra.

*Corresponding author. Electronic address: moustafa.elkurdi @ief.u-psud.fr

[1] C. G. Van De Walle and R. M. Martin, Phys. Rev. B **34**, 5621 (1986).

[2] S. Fukatsu and Y. Shiraki, Appl. Phys. Lett. **63**, 2378 (1993).

[3] D. C. Houghton, G. C. Aers, S.-R. Eric Yang, E. Wang, and N. L. Rowell, Phys. Rev. Lett. **75**, 866 (1995).

[4] M. Wachter, K. Thonke, R. Sauer, F. Schäffler, H. J. Herzog, and

E. Kasper, Thin Solid Films **222**, 10 (1992).

[5] T. Baier, U. Mantz, K. Thonke, R. Sauer, F. Schäffler, and H.-J. Herzog, Phys. Rev. B **50**, 15191 (1994).

[6] M. L.W. Thewalt, D. A. Harrison, C. F. Reinhart, J. A. Wolk, and H. Lafontaine, Phys. Rev. Lett. **79**, 269 (1997).

[7] R. People and J. C. Bean, Appl. Phys. Lett. **48**, 538 (1986).

[8] M. M. Rieger and P. Vogl, Phys. Rev. B **48**, 14276 (1993).

[9] O. G. Schmidt, K. Eberl, and Y. Rau, Phys. Rev. B **62**, 16715

(2000).

[10] G. L. Bir and G. E. Pikus, *Symmetry and Strain-Induced Effects in Semiconductors* (Halsted, New York, 1990).

[11] S. Richard, F. Aniel, and G. Fishman, Phys. Rev. B **70**, 235204 (2004).

[12] T. Fromherz, E. Koppensteiner, M. Helm, G. Bauer, J. F. Nützel, and G. Abstreiter, Phys. Rev. B **50**, 15073 (1994).

[13] M. El Kurdi, G. Fishman, S. Sauvage, and P. Boucaud, Phys. Rev. B **68**, 165333 (2003).

[14] A. I. Yakimov, N. P. Stepina, A. V. Dvurechenskii, and A. I. Nikiforov, and A. V. Nenashev, Phys. Rev. B **63**, 045312 (2001); see also J. H. Seok and J. Y. Kim, Appl. Phys. Lett. **78**, 3124 (2001).

[15] M. Cardona and F. Pollak, Phys. Rev. **142**, 530 (1966).

[16] R. Braunstein, Phys. Rev. **130**, 869 (1963).

[17] R. People, Phys. Rev. B **32**, 1405 (1985).

[18] J. P. Dismukes, L. Ekstrom, and L. J. Paff, J. Phys. Chem. **68**, 3021 (1964).

[19] G. Theodorou, P. C. Kelires, and C. Tserbak, Phys. Rev. B **50**, 18355 (1994).

[20] L. Colombo, R. Resta, and S. Baroni, Phys. Rev. B **44**, 5572 (1991).

[21] S. Richard, F. Aniel, G. Fishman, and N. Cavassilas, J. Appl. Phys. **94**, 1795 (2003).

[22] R. People, IEEE J. Quantum Electron. **22**, 1696 (1986).

[23] D. V. Lang, R. People, J. C. Bean, and A. M. Sergent, Appl. Phys. Lett. **47**, 1333 (1985).

[24] F. Schäffler, Semicond. Sci. Technol. **12**, 1515 (1997).

[25] P. D. Yoder, V. D. Natoli, and R. M. Martin, J. Appl. Phys. **73**, 4378 (1993).

[26] M. V. Fischetti and S. E. Laux, J. Appl. Phys. **80**, 2234 (1996).

[27] J. Weber and M. I. Alonso, Phys. Rev. B **40**, 5683 (1989).

[28] H. Sigg, C. V. Falub, E. Müller, A. Borak, D. Grützmacher, T. Fromherz, M. Meduna, and O. Kermarrec, Opt. Mater. **27**, 841 (2005).

[29] P. N. Keating, Phys. Rev. **145**, 637 (1966).

[30] G. Patriarche, I. Sagnes, P. Boucaud, V. Le Thanh, D. Bouchier, C. Hernandez, Y. Campidelli, O. Kermarrec, and D. Bensahel, Appl. Phys. Lett. **77**, 370 (2000).

[31] G. F. Koster, J. O. Dimmock, R. G. Weehler, and H. Statz, *Properties of the Thirty-Two Point Groups* (MIT Press, Cambridge, MA, 1963).

[32] A. Blacha, H. Presting, and M. Cardona, Phys. Status Solidi B **126**, 11 (1984).